Molecular Therapy
Oncology
Original Article

Enhancing antitumor efficacy of oncolytic virus M1 via albendazole-sustained CD8$^+$ T cell activation

Wenjing Bai,[1,2] Xia Tang,[1,2] Tong Xiao,[1,2] Yangyang Qiao,[1,2] Xuyan Tian,[1,2] Bo Zhu,[1,2] Jiehong Chen,[1] Chaoxin Chen,[1] Yuanyuan Li,[1] Xueying Lin,[1,2] Jing Cai,[1,3] Yuan Lin,[1] Wenbo Zhu,[1] Guangmei Yan,[1,4] Jiankai Liang,[1,2] and Jun Hu[1,2]

[1]Department of Pharmacology, Zhongshan School of Medicine, Sun Yat-sen University, Guangzhou 510080, China; [2]Department of Microbiology, Zhongshan School of Medicine, Sun Yat-sen University, Guangzhou 510080, China; [3]Department of Biochemistry, Zhongshan School of Medicine, Sun Yat-sen University, Guangzhou 510080, China; [4]Guangzhou Virotech Pharmaceutical Co., Ltd, #3 Lanyue Road, Science Park, Guangzhou 510663, China

The immune response plays a crucial role in the functionality of oncolytic viruses. In this study, Albendazole, an antihelminthic drug known to modulate the immune checkpoint PD-L1, was combined with the oncolytic virus M1 (OVM1) to treat mice with either prostate cancer (RM-1) or glioma (GL261) tumors. This combination therapy enhanced anti-tumor effects in immunocompetent mice, but not in immunodeficient ones, without increasing OVM1 replication. Instead, it led to an increase in the number of CD8$^+$ T cells within the tumor, downregulated the expression of PD1 on CD8$^+$ T cells, and upregulated activation markers such as Ki67, CD44, and CD69 and the secretion of cytotoxic factors including interferon (IFN)-γ, granzyme B, and tumor necrosis factor (TNF)-α. Consistently, it enhanced the *in vitro* tumor-killing activity of lymphocytes from tumor-draining lymph nodes or spleens. The synergistic effect of Albendazole on OVM1 was abolished by depleting CD8$^+$ T cells, suggesting a CD8$^+$ T cell-dependent mechanism. In addition, Albendazole and OVM1 therapy increased CTLA4 expression in the spleen, and the addition of CTLA4 antibodies further enhanced the anti-tumor efficacy *in vivo*. In summary, Albendazole can act synergistically with oncolytic viruses via CD8$^+$ T cell activation, and the Albendazole/OVM1 combination can overcome resistance to CTLA4-based immune checkpoint blockade therapy.

INTRODUCTION

Oncolytic viruses (OV) represent a fascinating class of viruses with the unique ability to selectively infect and destroy tumor cells while sparing normal healthy cells. These viruses not only directly target cancerous cells but also play a crucial role in triggering an anti-tumor immune response within the host organism.[1] However, despite their promise, challenges persist. One such obstacle arises from immunosuppressive molecules, which can hinder the effectiveness of oncolytic virus therapy. This negative feedback mechanism often diminishes the overall efficacy of virotherapy. For instance, the immunosuppressive effects of vascular endothelial growth factor (VEGF) go beyond the nutritional support of blood vessels, and involve suppressing dendritic cell maturation, impairing the recruitment and function of T cells, and recruiting regulatory T cells and bone marrow-derived suppressor cells that affect the expression of immune checkpoint molecules such as programmed death ligand 1 (PD-L1). These effects facilitate cancer immune evasion, revealing the complex role of VEGF in immune regulation. Our research has long verified that the oncolytic virus M1 (OVM1) has an effective killing effect on various types of tumors *in vivo* and *in vitro*.[2] However, we discovered that OVM1 can induce the expression of VEGF, which may compromise the anti-tumor efficacy of OVM1.[3,4]

Albendazole (ABZ) is a benzimidazole carbamate drug that has been used clinically for a long time to prevent and treat intestinal parasitic infections.[5] Recently, it has also been reported that ABZ has anti-cancer activity,[6] and its pro-apoptotic effect that depends on inhibiting tubulin polymerization may be the main mechanism of its anti-cancer effect.[7,8] However, some reports also suggest that ABZ has a significant role in anti-tumor immunity. Some articles have shown that ABZ can mediate the ubiquitination and degradation of PD-L1 in B16F10 and LLC tumor cells, and also enhance the activation of various immune cells in the body.[9] This is in line with its role in promoting Th2/Th1 switch in antiparasitic treatment.[10,11] Interestingly, studies have demonstrated that ABZ exerts anti-tumor effects on non-small cell lung cancer by lowering the activity of VEGF and PD-L1.[12]

We observed that the mRNA expression levels of *VEGF* and *CD274* were significantly increased in early tumor tissues treated with

Received 12 March 2024; accepted 1 May 2024;
https://doi.org/10.1016/j.omton.2024.200813.

Correspondence: Jiankai Liang, Zhongshan School of Medicine, Sun Yat-sen University, Guangzhou 510080, China.
E-mail: liangjk5@mail.sysu.edu.cn
Correspondence: Jun Hu, Zhongshan School of Medicine, Sun Yat-sen University, Guangzhou 510080, China.
E-mail: hujun@mail.sysu.edu.cn

OVM1 (Figures S1A and S1B). Thus, we examined the effect on cancer cells *in vitro*. We found that OVM1 alone could indeed elevate the expression of VEGF protein. In contrast, ABZ alone markedly suppressed the expression of VEGF in tumor cells. Moreover, ABZ could significantly reduce the expression of VEGF elevated by OVM1 (Figures S1C and S1D). Therefore, we attempted to enhance the efficacy of OVM1 by combining it with ABZ.

This study demonstrated that the combination of albendazole (ABZ) and Oncolytic Virus M1 (OVM1) significantly enhanced the anti-tumor effect of OVM1 in immunocompetent mice. Through the deletion of $CD8^+$ T cells and other experimental approaches, we discovered that the enhanced effect of the ABZ and OVM1 combination primarily relied on the infiltration and activation of $CD8^+$ T cells within the tumor microenvironment (TME). Furthermore, the addition of an anti-CTLA4 antibody achieved a better efficacy, suggesting a novel approach to overcome resistance to immune checkpoint blockers (ICB).

RESULTS

The combination of ABZ and OVM1 can enhance the anti-tumor efficacy of OVM1 *in vitro* by inducing cell apoptosis

We first evaluated whether the combination of OVM1 and ABZ enhances the inhibition of tumor cell viability *in vitro*. We performed an MTT assay on tumor cells treated with OVM1 or ABZ, and found that OVM1 alone can effectively inhibit the viability of GL261 or RM-1, and ABZ alone shows dose-dependent inhibition activity on these two cell lines (Figure 1A). The combination of ABZ further enhanced the inhibitory effect of OVM1 on both tumor cell lines in a dose-dependent manner (Figure 1A).

To study the mechanism of how ABZ enhances the anti-tumor efficacy of OVM1, we analyzed the apoptosis of tumor cells. The results show that OVM1 or ABZ alone can significantly increase the cleavage of Caspase-3 in both cell lines (Figures 1B and 1C). The combination treatment increased the cleavage of Caspase-3 more than OVM1 or ABZ alone (Figures 1B and 1C). We also measured the percentage of Annexin V/PI positive cells in tumor cells. The combination treatment with OVM1 and ABZ for 48 h significantly increased the percentage of Annexin V-positive cells more than OVM1 or ABZ alone in a dose-dependent manner (Figures 1D and 1E). These results suggest that both OVM1 and ABZ alone can induce tumor cell apoptosis, and their combination further enhances cell apoptosis.

Next, we further investigated the effects of OVM1 and ABZ on cancer cell proliferation using EdU assay. The results showed that OVM1 alone did not affect the EdU-positive proliferation in both cancer cell lines (Figure 1F). However, ABZ alone or in combination with OVM1 showed activity in inhibiting cancer cell proliferation in both cell lines (Figure 1F).

Our previous studies have shown that OVM1 replication in tumors plays a crucial role in the sustained killing efficacy on various cancers.[13] Therefore, we tested the effect of ABZ on virus replication and found that ABZ can significantly inhibit virus replication in RM-1 or GL261 (Figure 1G). The result that the combination of OVM1 and ABZ does not enhance viral replication poses a challenge to our attempts to use ABZ to enhance the oncolytic effect of OVM1 *in vivo*.

ABZ enhances the *in vivo* antitumor efficacy of OVM1 in a lymphocyte-dependent manner

To test whether the combination of ABZ and OVM1 can enhance the anti-tumor efficacy of OVM1 in immune-competent mice, we used C57BL/6 mice bearing subcutaneous tumors of RM-1 or GL261 and measured indicators such as survival time, tumor size, and T/C ratio to evaluate the anti-tumor effect. The administration process to tumor-bearing mice is shown in Figure 2A. The results showed that OVM1 alone could significantly inhibit tumor growth and extend the survival time of tumor-bearing mice, in both RM-1 (Figures 2B and S2A) and GL261 (Figures 2C and S2B) models. This is consistent with the results of previous studies in our laboratory.[14] And, combination of ABZ and OVM1 further enhanced these anti-cancer outcomes. We found that in the RM-1 (Figure 2D) or GL261 (Figure 2E) models, the T/C ratio after combined treatment of OVM1 and ABZ can be suppressed to below 40%, which is significantly better than using OVM1 alone. Consistent with this, we found that tumor volume and weight were significantly smaller and lighter in the group treated with the combination of ABZ and OVM1 compared with the group treated with OVM1 alone (data for RM-1 are shown in Figures 2F and 2G, data for GL261 are shown in Figures 2H and 2I). The above efficacy-related data in immune-competent mice indicate that the combination of ABZ and OVM1 show better anti-tumor efficacy than OVM1 alone. Furthermore, the liver and kidneys were not damaged as shown in the pathological data (Figure S2C), suggesting that the combination treatment did not cause additional toxic side effects.

Does this synergistic mechanism of ABZ involve increasing the virus replication in tumor tissues? We measured OVM1 viral genomic RNA in RM-1 and GL261 tumors and found that the combination of ABZ and OVM1 did not change the viral load in the tumors (Figure 2J). This result was in accordance with the finding that ABZ cannot enhance OVM1 virus replication in cell experiments *in vitro*.

Since it cannot be explained by promoting the replication of oncolytic viruses and enhancing direct oncolysis, we used athymic nude mice bearing RM-1 or GL261 tumors to further evaluate whether the enhancement of ABZ on the anti-tumor efficacy of OVM1 relies on the enhancement of anti-tumor immunity. The same grouping and administration methods were followed as in Figure 2A. The co-administration of ABZ and OVM1 is also safe in immunodeficient mice, comparable to that observed in immunocompetent mice, as the animals' body weights remained stable throughout the duration of the experiment, even when using immunodeficient mice (Figures S3A and S3B). More importantly, we found that OVM1 alone could significantly inhibit tumor growth, but the combination of ABZ and OVM1 did not futher improve the tumor inhibitory effect in either RM-1 (Figure 2K) or GL261 (Figure 2L) tumor-bearing nude mice models. ABZ treatment alone did not significantly extend median survival time in

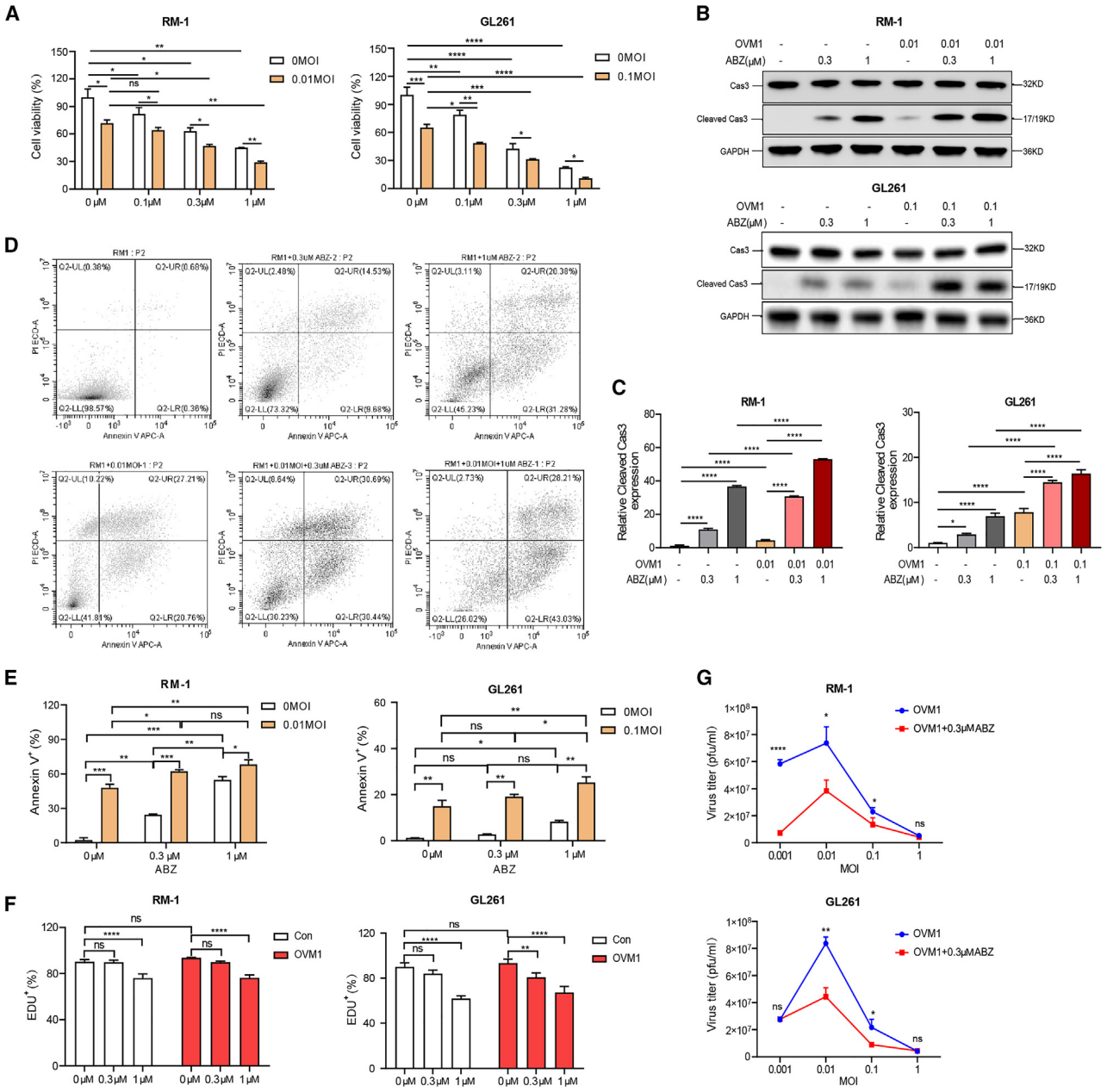

Figure 1. OVM1 combined with ABZ inhibited tumor cell growth *in vitro* by promoting apoptosis

(A) Cancer cells were treated with OVM1 and varying concentrations of ABZ (0.1, 0.3, 1 μM) for 48 h. Cell viability was then assessed by MTT assay. (B) Protein expression and cleavage of Caspase-3 were analyzed after 24-h treatment with OVM1 at different multiplicities of infection (MOIs) combined with varying ABZ concentrations. Band intensities were used for statistical analysis (Figure 1C). (D) Flow cytometry was used to determine the percentage of cells positive for Annexin V and propidium iodide (PI) (Figure 1E). (E) Proliferation of cancer cells was evaluated by the percentage of EdU-positive cells after 24-h treatment with OVM1 alone or combined with varying ABZ concentrations (Figure 1F). (G) Viral copy number was measured to assess OVM1 replication in tumor cells following treatment with 0.3 μM ABZ at 48 h post-infection at different MOI. Different cell lines were infected with OVM1 at varying MOI (0.01 for RM-1, 0.1 for GL261). Statistical significance is indicated: $^{*}p < 0.05$; $^{**}p < 0.01$; $^{***}p < 0.001$; $^{****}p < 0.0001$; ns, not significant.

nude mice bearing RM-1 (Figure S3C) and GL261 (Figure S3D) tumors. While ABZ also increased median survival time in nude mice to a statistically significant degree, the synergy of ABZ with OVM1 was relatively minimal in nude mice compared with immunocompetent mice. Unlike the experimental results in immune-competent mice, ABZ did not significantly enhance the anti-tumor efficacy of

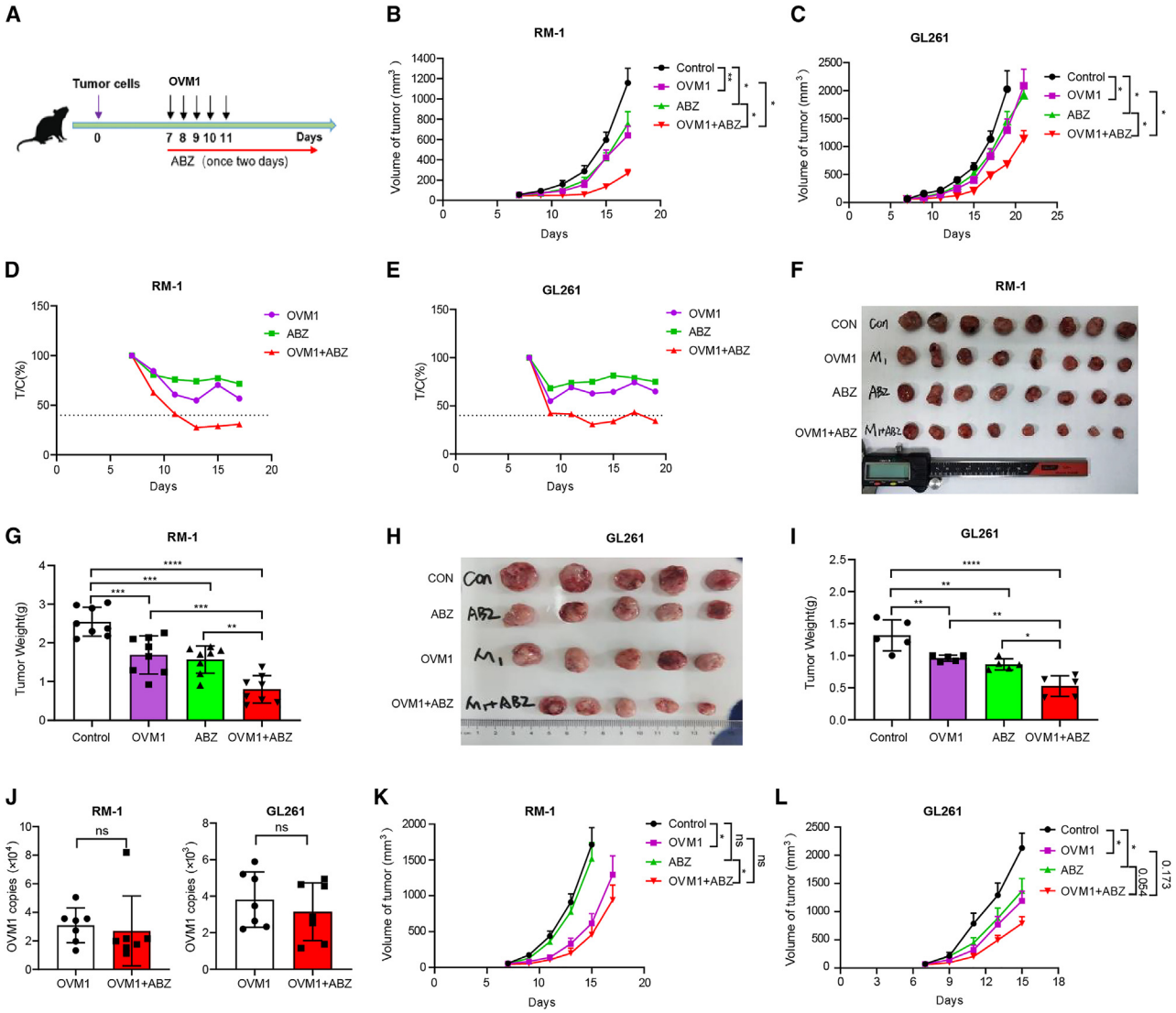

Figure 2. The combination of OVM1 and ABZ treatment significantly inhibits tumor growth

(A) Mice bearing tumor cells (RM-1 or GL261) subcutaneously on the right side were used for the experimental procedure according to the experimental flow chart. Nude mice for (K) and (L), and C57BL/6 mice for others. (B) The tumor growth curve of RM-1 tumors, $n = 6$ for the ABZ group and $n = 7$ for the other groups. (C) The tumor growth curve of GL261 tumors, $n = 7$. (D) The T/C (%) of RM-1 tumors treated with the combination of OVM1 and ABZ, $n = 6$ for the ABZ group and $n = 7$ for the other groups. (E) The T/C (%) of GL261 tumors, $n = 7$. T/C ratio of 40% is shown with a dotted line. (F) The tumor size when RM-1 tumors are treated with the combination of OVM1 and ABZ. $n = 8$. (G) The tumor weight of RM-1 tumors. $n = 8$. (H) The tumor size of GL261 tumors. $n = 5$. (I) The tumor weight of GL261 tumors. $n = 5$. (J) On day 7, the amount of viral replication in the tumor mice treated with the combination of OVM1 and ABZ. (K) The tumor growth curve of RM-1 tumors in nude mice treated with the combination of OVM1 and ABZ. $n = 6$. (L) The tumor growth curve of GL261 tumors in nude mice. $n = 6$. Statistical significance is represented by an asterisk, where * represents $p < 0.05$, ** $p < 0.01$, *** $p < 0.001$, **** $p < 0.0001$, and 'ns' represents no statistical significance.

OVM1 in immune-deficient mice. These results suggest that lymphocyte-mediated anti-tumor immunity is likely necessary for the enhancement of ABZ on OVM1 anti-tumor efficacy.

ABZ increases CD8$^+$ T cell count and activity in the tumor immune microenvironment during OVM1 oncolytic virotherapy

We aimed to clarify the immune mechanism behind ABZ's improved anti-tumor effect on OVM1. To do this, we analyzed immune cells in the TME, spleen, and peripheral blood of mice bearing subcutaneous RM-1 tumors, using flow cytometry. Our findings indicate that the combined treatment with ABZ significantly increases the number of T cells in the tumor during OVM1 treatment, particularly CD8$^+$ T cells (Figure 3A). In line with this, ABZ enhances the number of Ki67$^+$ CD8$^+$ T cells in the tumor during OVM1 treatment (Figure 3B), a phenomenon not clearly observed in CD4$^+$ T cells (Figures S4A and S4B). These results suggest that ABZ may promote the proliferative

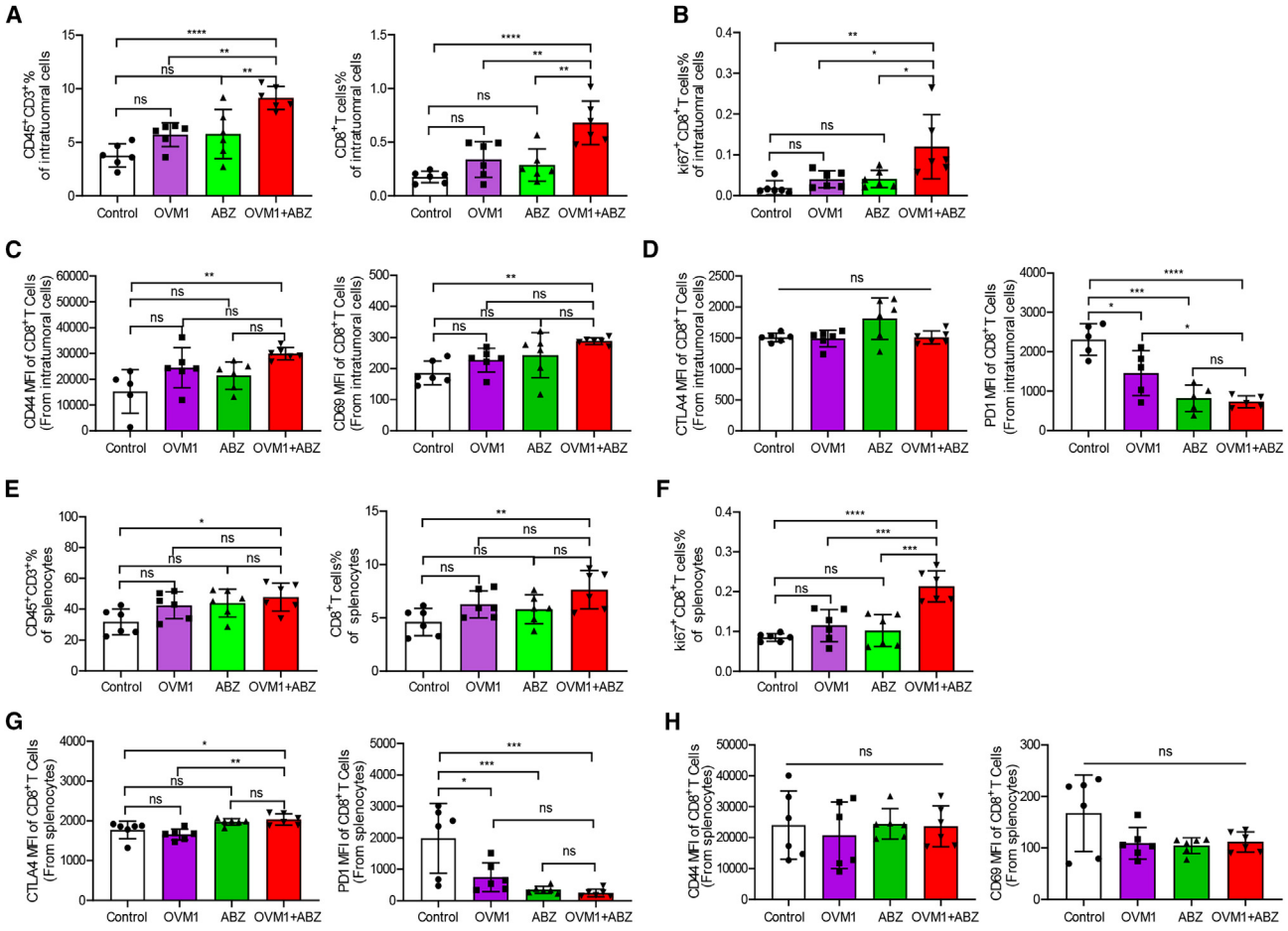

Figure 3. In combination with ABZ, there was an increase in intratumoral CD8⁺ T cells in C57BL/6 mice treated with OVM1

The RM-1 tumor cells were subcutaneously transplanted into mice. The first day of OVM1 administration, which was designated as day 1. On day 10, the mice were euthanized, and tumor tissues or spleens were collected, $n = 6$. The proportion of $CD45^+CD3^+$ T and $CD8^+$ T cells within tumor (A) or spleen (E). The proportion of $ki67^+CD8$ T cells within tumor (B) or spleen (F). The mean fluorescence intensity of CD44 and CD69 within tumor (C) or spleen (H). The mean fluorescence intensity of CTLA4 and PD1 within tumor (D) or spleen (G). Statistical significance is represented by an asterisk, where $^*p < 0.05$, $^{**}p < 0.01$, $^{***}p < 0.001$, $^{****}p < 0.0001$, and "ns" represents no statistical significance.

$CD8^+$ T cells increasing in the tumor during OVM1 treatment. Consistently, the expression of CD44 and CD69 was markedly increased in $CD8^+$ T cells of mice after treatment with a combination of ABZ and OVM1 (Figure 3C), while the expression of PD1 was significantly reduced (Figure 3D), which together indicates an improvement in the function of $CD8^+$ T cells in the TME. But, there was no change in CTLA4 in these cells (Figure 3D).

Additionally, we examined the proportions of other types of immune cells in tumors and found that the proportion of Treg cells in each group of mice did not significantly change compared with the untreated group (Figure S4C). As depicted in Figure S4D, combined treatment with ABZ significantly increased intratumoral $CD11b^+$ cells compared with OVM1 treatment alone (Figure S4D). We found that while the proportion of macrophages did not change significantly, the expression of polarization markers CD80 and CD163 in macrophages was significantly downregulated after the combined use of ABZ and OVM1 compared with treatment with OVM1 alone (Figure S4E), suggesting the inhibition of tumor-associated macrophages. Previous literature has reported that ABZ can reduce the expression of the inhibitory immune molecule PD-L1 in tumor cells.[9] Contrarily, we found that the combined treatment with OVM1 and ABZ significantly upregulated PD-L1 expression in $CD45^-$ non-immune cells compared with control group (Figure S4F). Furthermore, combined treatment with ABZ did not affect PD-L1 expression in tumor-associated macrophages (data not shown).

As the largest peripheral immune organ in the human body, the spleen plays a crucial role in the body's defense system, particularly in anti-tumor immunity.[15] Consequently, we further investigated the proportion of T cells in the spleen and discovered that combined treatment with ABZ did not influence the proportion of T cells,

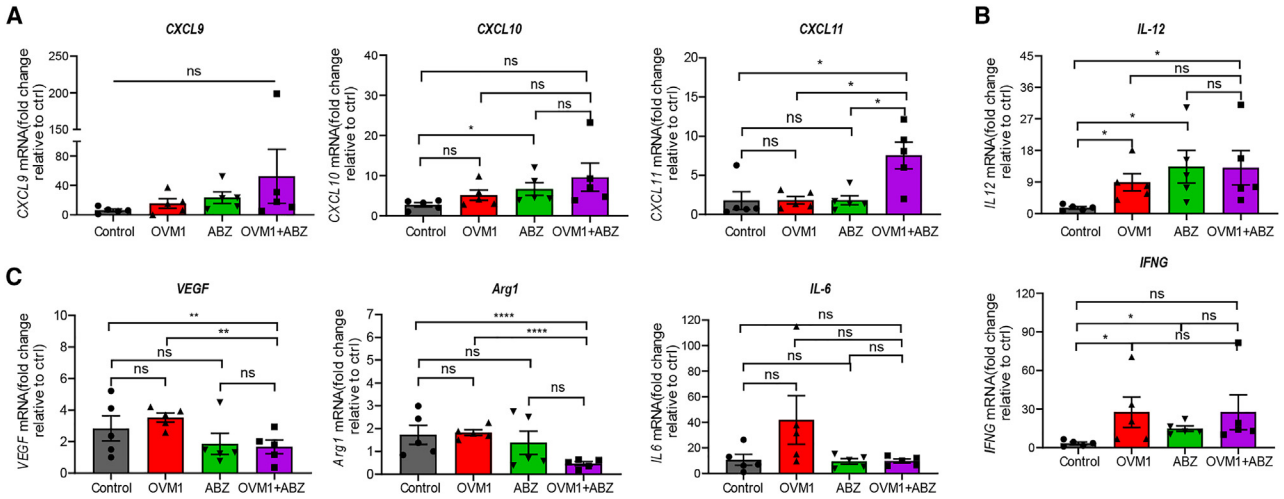

Figure 4. ABZ can modulate the expression of anti-tumor immunity-related genes in the tumor tissues of C57BL/6 mice treated with OVM1

The RM-1 tumor cells were subcutaneously transplanted into the mice. The first day of OVM1 and ABZ administration was designated as day 1. On day 10, the mice were euthanized, and tumor tissues or spleens (n = 5) were harvested and RNA was extracted, RT-PCR was performed to evaluate the mRNA level of T cell-associated chemokines (A), the mRNA levels of T cell activation-associated genes, including *IL-12* or *IFNG* (B) and the mRNA levels of immune suppression-associated genes, including *VEGF*, *Arg1,* and *IL-6* (C). Statistical significance is represented by an asterisk, where * represents $p < 0.05$, ** $p < 0.01$, **** $p < 0.0001$, and "ns" represents no statistical significance.

$CD8^+$ T, or $CD4^+$ T cells in the spleen during OVM1 treatment (Figures 3E and S4G). However, the proportion of $Ki67^+$ cells among $CD4^+$ T or $CD8^+$ T cells significantly increased after combined treatment with ABZ (Figures 3F and S4H). Moreover, the proportion of Treg cells in the spleen also significantly increased after combined treatment with ABZ (Figure S4I). In line with this, combination treatment also upregulated the expression of the immune checkpoint molecule CTLA4 (Figure 3G). Similar to the situation in the tumor microenvironment, the expression of the exhaustion indicator molecule PD1 was significantly reduced in $CD8^+$ T cells in the spleen after combined treatment with ABZ (Figure 3G). However, activation markers CD44 and CD69 did not exhibit significant changes (Figure 3H).

We also measured the proportion of T cells in peripheral blood. The results indicated that the proportion of T cells in the blood was consistent with the phenomenon observed in the spleen after combination treatment compared with treatment with OVM1 alone (Figures S5A and S5B). However, there were no significant differences in the proportion of Treg cells in the blood between these two groups (Figures S5C and S5D).

In summary, during OVM1 treatment, combined treatment with ABZ can stimulate an increase in the number of T cells in the tumor microenvironment, particularly $CD8^+$ T cells. The detection results of molecular markers suggest that combined treatment with ABZ can reduce exhaustion (PD1) of $CD8^+$ T cells in the tumor, and promote their proliferation (Ki67) and activation (CD44 and CD69). The spleen exhibited an increase in Treg and CTLA4, along with an unchanged proportion of T cells and stable levels of activation markers such as CD44 and CD69. This suggests the existence of negative feedback regulation within the spleen secondary to excessive activation of immune cells.

ABZ can optimize the pattern of gene expression associated with anti-tumor immunity in tumor tissues during OVM1 virotherapy

Chemokines and cytokines play crucial roles in anti-tumor immunity. Consequently, we analyzed the mRNA expression of these kinds of genes in tumors. Our findings revealed that, with the exception of ABZ treatment alone, which increased the expression level of *CXCL10*, neither OVM1 treatment alone nor ABZ treatment alone can affect the expression of T cell-related chemokines detected by us (Figure 4A). However the combination treatment with ABZ notably enhanced *CXCL11* expression during OVM1 treatment (Figure 4A). CXCL11 is a more potent CXCR3 ligand than CXCL9 and CXCL10. Interleukin (IL)-12 can exert anti-tumor effects by inducing T cells to produce IFN-γ.[16] We examined the mRNA expression of *IL-12* and *IFNG* and discovered that either OVM1 or ABZ treatment alone can enhance the expression of *IL-12* or *IFNG*. However, the combined treatment did not further elevate the expression levels of these two genes (Figure 4B). Numerous studies have reported that IL-6 is associated with the progression and drug resistance of various cancers.[17,18] Consequently, we assessed *IL-6* expression in tumor tissues and observed that OVM1 treatment alone tended to upregulate *IL-6*, a finding that aligns with our studies in other tumors.[18] Although *IL-6* demonstrated a trend toward reduction after 10 days of combined treatment with ABZ and OVM1, this decrease was not statistically significant when compared with the treatment with OVM1 alone (Figure 4C).

Additionally, we evaluated the mRNA expression of other immune-related genes in tumor tissues, such as *arginase 1* (*Arg1*), *CD274,* and *VEGF*. Arg1 in tumors is typically produced by MDSC, which can suppress T cell responses in tumor patients, thereby facilitating tumor progression.[19,20] Our results indicated that neither OVM1 treatment alone nor ABZ treatment alone influenced the expression of *Arg1*, but their combination significantly diminished the expression level of *Arg1* in tumor tissues (Figure 4C). This outcome aligns with the observed reduction in M2 polarization of macrophages detected by flow cytometry, suggesting enhanced anti-tumor immunity in tumor-associated myeloid cell populations (Figure S4E). Prior studies have demonstrated that OVM1 treatment can elevate the expression of *CD274* and *VEGF*, both of which are adverse to anti-tumor effects. Literature reports suggest that ABZ can inhibit PD-L1 and VEGF in tumor cells, thereby exerting anti-tumor effects.[9,12] However, we discovered that combined treatment with ABZ did not impact *CD274* expression in the tumor tissue (data not shown), same as the expression in $CD45^-$ cells (Figure S4F) or tumor-associated macrophages using flow cytometry (data not shown). But, combined treatment with ABZ significantly suppressed *VEGF* expression in tumor tissues during OVM1 treatment (Figure 4C), which is in line with our previous *in vitro* cytology experimental results (Figure S1C). Among the two reported anti-tumor targets of ABZ, namely PD-L1 and VEGF, it can be inferred that ABZ enhances the anti-tumor effect of OVM1 mainly by downregulating the expression of VEGF rather than PD-L1.

ABZ enhances the tumoricidal toxicity of lymphocytes during OVM1 oncolytic virus treatment

Subsequently, we aimed to determine whether the combined treatment with ABZ truly augmented the anti-tumor immune activity of T cells in mice, utilizing *in vitro* detection of lymphocyte tumoricidal toxicity and monitoring of immunotoxic factor secretion during the immune killing process.

On the 10th day following the treatment on the subcutaneously transplanted tumor-bearing mice (bearing RM-1 or GL261), we harvested lymphocytes from the spleen and tumor-draining lymph nodes (TDLNs), and co-cultured them with the same tumor cells as used *in vitro* for up to 48 h (Figure 5A). Subsequently, the viability of tumor cells was assessed by an MTT assay to evaluate the tumoricidal toxicity of the lymphocytes (Figure 5A). OVM1 treatment alone demonstrated a significant ability to enhance the tumoricidal toxicity of lymphocytes derived from mice samples (Figures 5B and 5C). And, after combined treatment, nearly all lymphocyte samples exhibited further enhanced tumoricidal toxicity compared with OVM1 or ABZ treatment alone, and in an E:T ratio-dependent manner (Figures 5B and 5C). This result reaffirmed the activation effect of ABZ on the immune activity of lymphocytes.

IFN-γ and granzyme B are widely recognized as the primary immunotoxic factors that lymphocytes utilize to attack tumors. We employed an enzyme-linked immunosorbent assay (ELISA) to detect the secretion of these two factors in the co-culture supernatants of all groups during the immune-mediated tumor killing process. Our findings revealed an elevated secretion of granzyme B and IFN-γ by lymphocytes derived from RM-1 tumor-bearing mice treated solely with OVM1 (Figures 5D and 5E), compared with the control group. Notably, this secretion was further augmented during the procedure of co-culture of lymphocytes derived from the mice accepted combined treatment (Figures 5D and 5E).

TNF-α is another potent factor that can directly eliminate tumor cells by inducing apoptosis.[21] Interestingly, while lymphocytes derived from mice treated with ABZ did not show a significant difference in TNF-α secretion compared with the control group, there was a significant enhancement of TNF-α expression in the lymphocytes derived from mice treated with a combination of OVM1 and ABZ, compared with those treated with OVM1 alone (Figures 5D and 5E).

In summary, these results suggest that OVM1 treatment alone can effectively stimulate the tumoricidal immunotoxicity of both local and systemic lymphocytes in tumor-bearing mice. Furthermore, the combined treatment of OVM1 and ABZ can further enhance this immunotoxicity. This enhancement may be mediated by secreted immunotoxic factors, such as granzyme B, IFN-γ, and TNF-α, etc.

The enhancement of OVM1 anti-tumor efficacy by ABZ is $CD8^+$ T cell dependent

It has been mentioned that the anti-tumor effect of OVM1 enhanced by ABZ in immunocompetent mice (Figure 2) is much stronger than the therapeutic effect in immunodeficient mice (Figure S3). This suggests that the immune activity of lymphocytes plays a very important role in combination enhancement of ABZ. ABZ increased the number of intratumoral $CD8^+$ T cells during OVM1 treatment and boosted the cytotoxicity of lymphocytes and the production of immunotoxic factors (Figures 3 and 5). $CD8^+$ T cells mediate effective anti-tumor function and play a key role in immunotherapy-induced anti-cancer immune responses.[22] To test the role of $CD8^+$ T cells in the combination therapy, we used CD8 antibody to deplete them in immunocompetent C57BL/6 mice and evaluated the impact on the anti-tumor efficacy of OVM1. First, we assessed the depletion efficiency of $CD8^+$ T antibodies in mice. Flow cytometry results revealed that $CD8^+$ T cells in tumor, spleen, and peripheral blood were nearly eliminated after $CD8^+$ T antibody treatment (Figure 6A). Next, we measured the tumor size *in vivo* and the survival time of tumor-bearing animals to evaluate the anti-tumor efficacy in mice.

Compared with the immunoglobulin (Ig)G2b group, $CD8^+$ T cell depletion significantly accelerated tumor growth (Figures 6B and 6C). However, we observed that $CD8^+$ T cell depletion only slightly increased the tumor volume in RM-1 tumor-bearing mice treated with OVM1 alone, and the difference was not significant (Figure 6D).

Differently, $CD8^+$ T cell depletion significantly enlarged the tumor size in tumor-bearing mice treated with ABZ alone, reaching a level similar to that of untreated mice, and almost completely eliminated the survival extension effect (Figures 6B–6D). This result demonstrates that the anti-tumor effect of ABZ alone depends on $CD8^+$ T

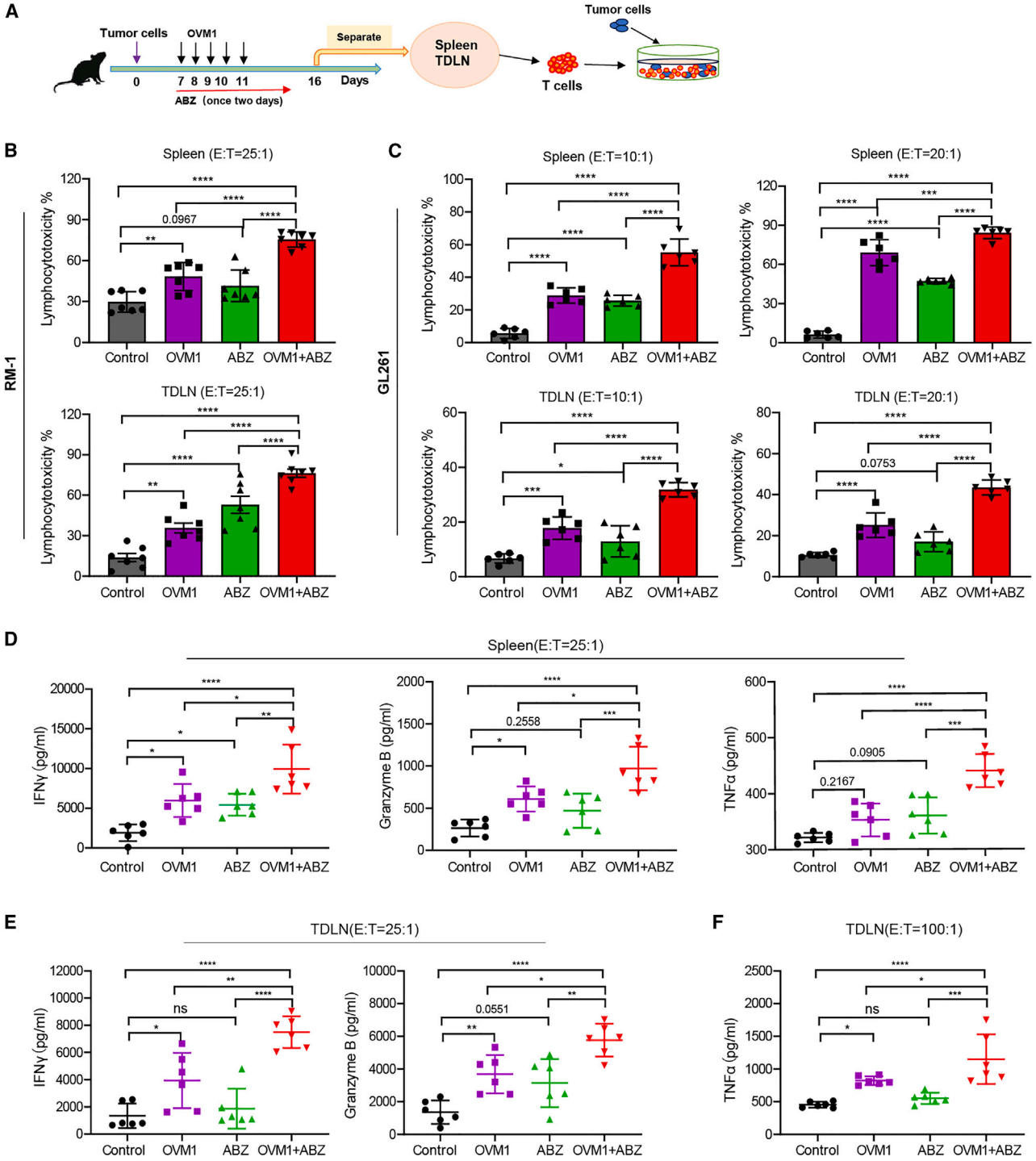

Figure 5. The combination of OVM1 and ABZ enhances the lymphocytes' tumor-killing effect

The RM-1 tumor cells were subcutaneously transplanted into the mice. The first day of OVM1 and ABZ administration was designated as day 1. On day 10, the mice were euthanized, the spleen or draining lymph nodes were harvested, and lymphocytes were isolated. These lymphocytes were co-cultured with the same type of tumor cells as the animal model at a certain E/T ratio shown (E:T = 100, 25, 20, and 10). (A) After 48 h, the supernatant was collected. (B and C) The MTT assay was used to detect the tumoricidal toxicity of the lymphocytes. $n = 6$. (D–F) The secretion of cytotoxic factors IFN-γ, granzyme B, and TNF-α in the supernatant was measured. $n = 6$. Statistical significance is represented by asterisks, where * represents $p < 0.05$, ** $p < 0.01$, *** $p < 0.001$, **** $p < 0.0001$, and "ns" represents no statistical significance.

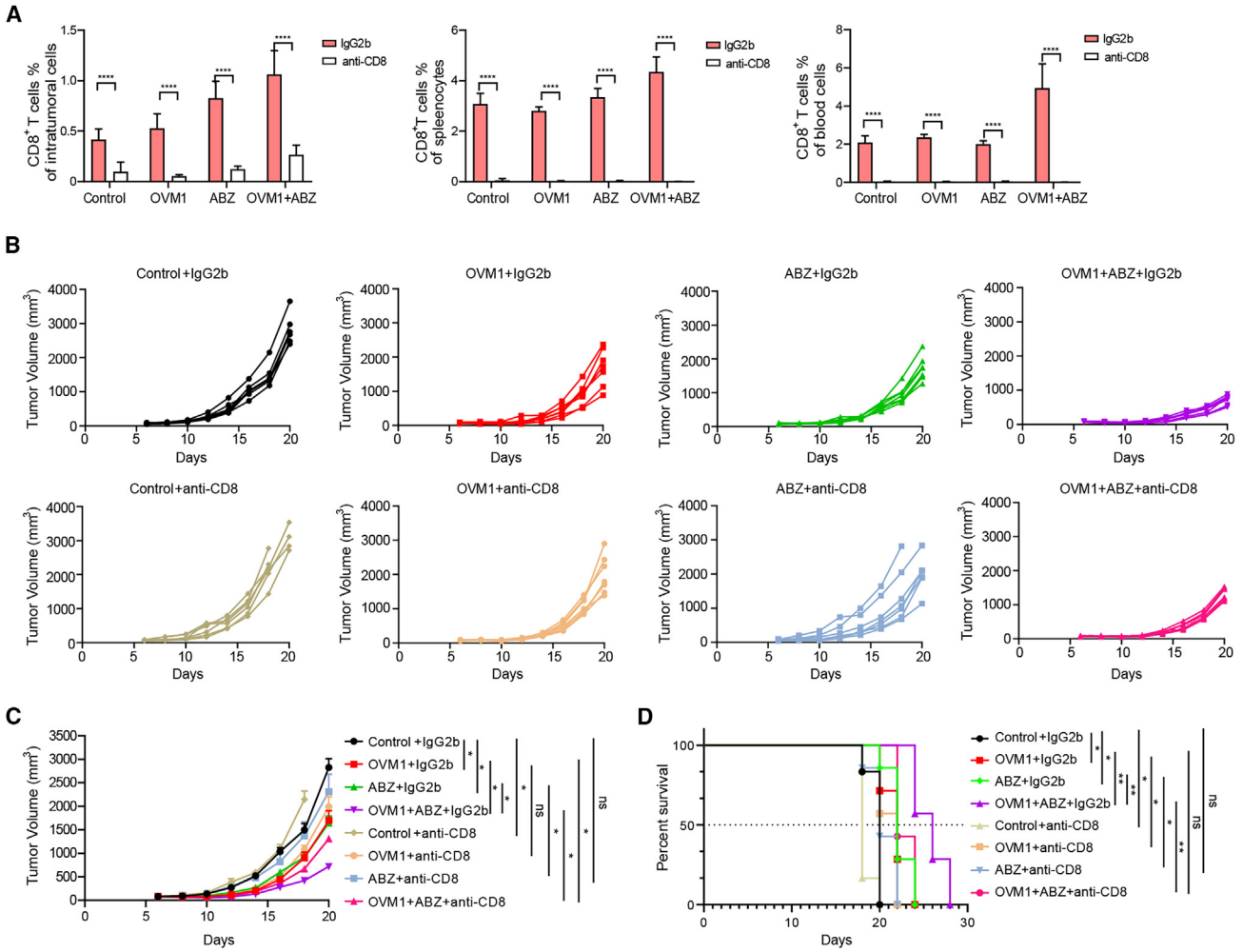

Figure 6. Enhancement of OVM1's anti-tumor efficacy by ABZ depends on CD8⁺ T Cells

When the tumor size reached between 50 mm^3 and 100 mm^3, each mouse was intraperitoneally administered with either CD8 antibody or an isotype control antibody every 3 days. The day of the first antibody injection is designated as day 0. Starting from day 1, an intravenous injection of the OVM1 virus was administered. Additionally, an intraperitoneal injection of albendazole at a dose of 50 mg/kg was administered every other day beginning from day1. On day 10, samples were collected from the mice, including tumors, spleens, and peripheral blood. The Control+IgG2b group and the Control+Anti-CD8 group each consisted of six mice. The six other groups each consisted of seven mice. (A) Flow cytometry was employed to analyze the $CD8^+$ T cells in different groups ($n = 3$) of total cells. (B) Tumor growth curves for each mouse ($n \geq 6$). (C and D) Tumor growth curve and survival curves of different groups of mice ($n \geq 6$). Statistical significance is denoted by an asterisk, where * represents $p < 0.05$, ** $p < 0.01$, **** $p < 0.0001$, and "ns" indicates no statistical significance.

cells. Likewise, $CD8^+$ T cell depletion nearly nullified the expected improvement of the antitumor efficacy of OVM1 enhanced by ABZ in combination-treated mice (Figures 6B–6D). These results suggest that the enhanced anti-tumor effect of OVM1 enhanced by combination treatment with ABZ also depends on $CD8^+$ T cells.

OVM1 combined with ABZ can overcome CTLA4 resistance

High expression of immune checkpoint molecules determines good clinical response to ICB treatment.[23] As stated above, OVM1 combined with ABZ did not affect the expression of CTLA4 on T cells in the TME, but significantly increased it in the spleen (Figures 3D and 3G). Therefore, we treated tumor-bearing mice with CTLA4 antibody in combination with OVM1 and ABZ to test whether ABZ-enhanced OVM1 can boost the effects of ICB as a whole. The results showed that CTLA4 antibody alone had a poor therapeutic effect on RM-1 tumor-bearing mice, with no significant difference in tumor size and median survival time, indicating that RM-1 tumors were insensitive to CTLA4 antibody treatment (Figure 7), similar to the ICB resistance that occurs frequently in clinical practice. However, after combined treatment with "OVM1+ABZ," the tumor size of RM-1 tumor-bearing mice was significantly smaller, and the survival time of the mice was significantly longer (Figure 7). This suggests that "OVM1+ABZ" can be used as a modality to increase the sensitivity of resistant

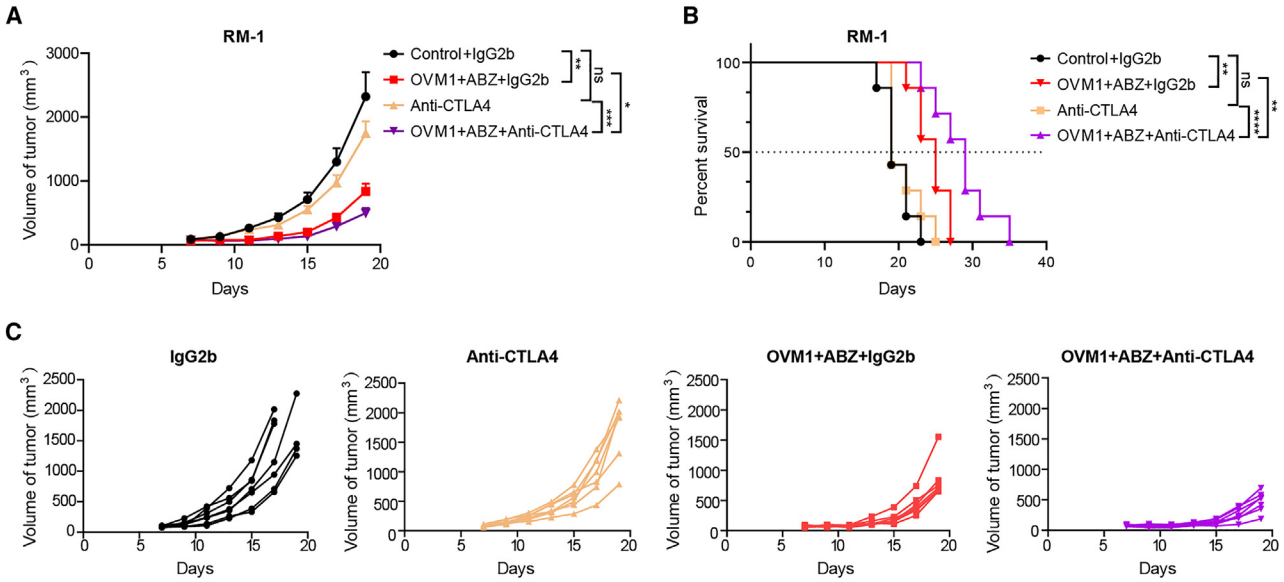

Figure 7. The combination of OVM1 and ABZ can mitigate CTLA4 resistance

Once the tumor size ranged from 50 mm^3 to 100 mm^3, each mouse was intraperitoneally administered with 200 μg of CTLA4 antibody or isotype control antibody on day 1, and then once every 3 days. On the first day, 300 μL of OVM1 (3×10^6 pfu) was administered intravenously each day for a total of 5 days, and 50 mg/kg of albendazole was administered intraperitoneally every other day. (A) Tumor growth curves of different groups of RM-1-bearing mice, $n = 7$. (B) RM-1 tumor survival curve of RM-1-bearing mice, $n = 7$. (C) Tumor growth curves for each mouse, $n = 7$. Statistical significance is indicated by an asterisk, $^*p < 0.05$, $^{**}p < 0.01$, $^{***}p < 0.001$, $^{****}p < 0.0001$, "ns" for no statistical significance.

cancer to CTLA4 antibody treatment, offering a solution for overcoming CTLA4 treatment resistance.

DISCUSSION

With the deeper understanding of cancer pathology, cancer therapeutic methods have diversified. The oncolytic virus therapy has emerged as an anti-tumor therapy with its unique features of targeted oncolytic killing and immune activation, offering new hope for the cure of tumors.[24–26] The natural oncolytic virus M1 achieves high safety and efficacy by selectively replicating and destroying tumor cells that lack zinc finger antiviral protein (ZAP), without harming normal cells.[27] It is regarded as a novel oncolytic virus with great development potential. However, due to the complexity and heterogeneity of tumor biology, single treatment has limited effectiveness in treating tumors. Therefore, using combination therapy is a reasonable strategy to improve the efficacy of anti-tumor therapy. This study explored the potential of combining OVM1 and ABZ for cancer therapy. Our findings demonstrate that the combination treatment resulted in a synergistic anti-tumor effect in immunocompetent mice, leading to improved survival time and reduced tumor growth.

Oncolytic viruses need immune activation to achieve their anti-tumor effects.[28] However, immune activation is hard to maintain well by acute viral infection. Therefore, combining oncolytic viruses with other cancer treatments such as chemotherapy, radiotherapy, immunotherapy, or cell therapy can enhance the outcomes.[18,25,29] Previous studies have shown that OVM1 treatment alone can significantly increase the expression of *CD274* and *VEGF*, which may compromise the efficacy of anti-tumor immunity. Therefore, overcoming these limitations is crucial for the oncolytic virus OVM1 therapy.

We found that ABZ has an inhibitory effect on the replication of viruses in tumor cells *in vitro*, which may result from its ability to inhibit tumor cell proliferation. However, ABZ did not significantly affect virus replication *in vivo*.

Moreover, in RM-1 tumor-bearing mice, OVM1 and ABZ combination had a significant increased anti-tumor effect in immunocompetent mice, but had almost no similar effect in immunodeficient mice (Figure 2). In a GL261 immuno-competent mouse model, we found that OVM1 alone significantly inhibited tumor growth and extended the median survival time. Compared with OVM1 monotherapy, combination therapy further inhibited GL261 tumor growth, significantly extended the median survival time. In GL261 tumor-bearing mice model, the combination treatment had a better antitumor effect in immunocompetent mice (Figures 2B and 2C) than in immunodeficient mice (Figures 2K and 2L). However, the synergistic contribution of ABZ in GL261 tumor-bearing mice is less than ideal compared with that in RM-1 tumor-bearing mice, especially in terms of survival. The details need to be further clarified.

We investigated the mechanism of the combined treatment and found that it stimulated the secretion of IFN-γ, granzyme B, and TNF-α from lymphocytes originating from the spleen and TDLN of tumor-bearing

mice. It also increased the tumoricidal activity of T cells in co-culture experiments. Moreover, when we treated RM-1 tumor-bearing mice with OVM1, adding ABZ enhanced the number and activity of T cells in the tumor. This could be due to ABZ either facilitating T cell proliferation or preventing T cell exhaustion. Some evidence supports the former hypothesis, such as the significant rise of Ki67 positive rate in $CD8^+$ T cells induced by ABZ. Other evidence supports the latter hypothesis. For instance, ABZ reduced the expression of PD1 and increased the expressions of CD44 and CD69 in $CD8^+$ T cells.

Furthermore, the combination therapy elevated the expression of the chemokine *CXCL11* in RM-1 tumors, which suggests another potential mechanism for the augmentation of T cells within the tumor, namely, the enhancement of T cell migration and infiltration. VEGF is known to exert a significant influence on T cells. Prior studies have shown that VEGF can hinder T cell recruitment by disrupting the TNF-α/CXCL11.[4,30] This aligns with our experimental findings where combination therapy reversed the OVM1-induced elevation of *VEGF* mRNA expression in tumor tissues.

Interestingly, VEGF can also inhibit the expression of PD-1 on the T cell surface and promote their proliferation, ultimately enhancing their anti-tumor function.[3,31] These observations are strongly supported by our findings that treatment combined with ABZ suppresses VEGF expression in tumors, inhibits PD-1, and enhances Ki-67 proliferation in $CD8^+$ T cells within both tumors and the spleen during OVM1 therapy. Collectively, these results suggest that ABZ may enhance the anti-tumor function of T cells during OVM1 therapy by inhibiting the secretion of VEGF by tumor cells.

We also found that ABZ did not significantly alter the proportions of Treg cells or macrophages in the tumor microenvironment. However, we observed an increase in the proportion of CD11b-positive cells in the tumor tissue, indicating that the combination therapy enhanced the infiltration of some unknown types of immune cells other than macrophages. These cells may also contribute to the improved anti-tumor efficacy of ABZ. Furthermore, the combination treatment markedly reduced the mRNA expression level of *Arg1* in tumor tissues. In line with this, the expression of CD163 was also diminished, which implied that the immunosuppressive phenotype of tumor-associated macrophages was reversed.

ICBs, which target immune checkpoints such as PD-1, PD-L1, or CTLA-4 and prevent cancer cells from escaping the host immune response, have emerged as one of the key cancer treatments.[32,33] Although ICB has held great promise for cancer treatment, the efficacy of ICB only benefits a minority of patients, which is due to the low response rates.[34] In this study, we found that the combination of OVM1 and ABZ can improve the therapeutic effect of CTLA4 antibody in a drug-resistant tumor model. Notably, our results implied that the enhanced therapeutic efficacy appeared to be mediated by $CD8^+$ T cells.

Unlike our previous discovery of enhancing direct oncolytic killing of tumor cells by stimulating cAMP/Epac1, ABZ enhances the immune system's attack on tumors *in vivo*.[32] Mechanistically, ABZ seems to influence the tumor microenvironment in a way that promotes infiltration, proliferation, and function of $CD8^+$ T cells. This effect could be due to a complicated mechanism, including VEGF, PD-1, Ki67, CXCL11, Arg1, and other molecules. However, further studies are required to fully understand the specific molecular pathways by which ABZ modulates $CD8^+$ T cell activity.

It's important to note that this study was limited to two tumor models (RM-1 and GL261). Further evaluation across a wider range of tumor types is necessary to determine if these findings can be generalized.

In conclusion, this study suggests that the combination of OVM1 and ABZ shows promise as a potential therapeutic approach for cancer, particularly in tumors that resist current immunotherapies. Future investigations should focus on elucidating the specific mechanisms of action and evaluating the efficacy of this combination therapy across a broader range of tumor types.

MATERIALS AND METHODS

Cell lines and cell culture

The RM-1 mouse prostate cancer cell line was purchased from Guangzhou SaiKu Biotechnology Co., Ltd., and GL261 was purchased from Tianjin Medical University. Cells were cultured in a 37°C incubator (Thermo Fisher, USA) containing 5% CO2, using 1640 (C11875500BT, Gibco) for RM-1, or DMEM (C11995500BT, Gibco) for GL261, and 100 μg/mL penicillin-streptomycin (SV30010, HyClone) and 10% FBS (10091148, Gibco) were added to the culture medium.

Viruses and drugs

The OVM1-GFP used in *in vitro* experiments is a virus strain loaded with independently expressible jellyfish green fluorescent protein (GFP) in wild-type alphavirus M1. OVM1 used in *in vivo* experiments was provided by Guangzhou Virotech Pharmaceutical Technology Co., Ltd. Albendazole was purchased from MCE with the product number HY-B0223.

Cell viability analysis

The 3-(4,5-dimethylthiazole-2-yl)-2,5-diphenyltetrazoli bromide (MTT) assay was used to detect cell metabolic activity as an indicator of cell viability. Cells were washed twice with phosphate-buffered saline (PBS) and incubated with MTT for 2 h. The absorbance value of each well was measured at OD490 nm using ELISA (BioTek, USA) to determine cell viability. Survival rate (%) was calculated using the following formula: (absorbance of the experimental group − background absorbance)/(absorbance of the control group − background absorbance) × 100%.

Virus titer

Take BHK-21 cells in the logarithmic growth phase and place them on a 96-well plate. The supernatant containing the virus in serum-free medium was diluted at a ratio of 10 times, with a minimum dilution ratio of 10^6; a 20-μL sample diluent was added to each well,

eight replicate wells were set up for each dilution, and eight replicate wells were also set up for the control group. The condition of cellular lesions and GFP green fluorescence signal was observed daily. After 72 h of infection, the number of wells with green fluorescence at each dilution was recorded based on the GFP signal. Virus titers were calculated using the Improved–Kärber method with the calculation formula: logTCID50 = log(highest dilution giving 100% GFP positive) − log(dilution factor) × (∑infected rate at each dilution − 0.5).

Cell proliferation analysis

5-Ethynyl-2′- deoxyridine (5-EdU) is a thymidine analog that can be incorporated into replicating DNA for detection of cell proliferation. After OVM1 and ABZ treatment, cells were incubated with 100 μL 50 μM EdU for 2 h and washed twice with PBS. Then, after incubating for 30 min in 50 μL of fixation solution (PBS containing 4% paraformaldehyde), the supernatant was discarded. Then, incubated with 50 μL of 2 mg/mL glycine for 5 min and washed with PBS. Then, 100 μL Permeabilization buffer (0.5% Triton X-100 PBS) was added, incubated for 10 min, and then washed with PBS. Then, incubated in 100 μL Apolo staining solution for 30 min in the dark, and treated with 100 μL Permeabilization buffer for 10 min, repeated twice, and the supernatant was discarded. Then, incubated in 100 μL Hoechst33342 for 30 min in the dark and washed three times with PBS. Finally, cells were detected using a flow cytometer (Beckman Coulter, USA) in 200 μL PBS.

Apoptosis analysis

To evaluate cell apoptosis, cells with OVM1 and different concentrations of ABZ (0.3 μM and 1 μM) *in vitro* for 48 h, cells were washed with PBS. Cells were resuspended in buffer and stained with Annexin V (0.6 mg/mL) and propidium iodide (PI) (5 mg/mL) at room temperature using Apoptosis Detection Kit (AT107-100, Lianke Biotech) for 5 min before Flow cytometry analysis.

Western bloting

Cells were washed with cold PBS and lysed with RIPA. The total protein was separated by sodium dodecyl sulfate polyacrylamide gel electrophoresis (SDS-PAGE), and then transferred to nitrocellulose membrane (horizontal cutting membrane). Next, immunoblotting was performed on the membrane using the following antibodies: Caspase-3 Antibody (# 9662S, Cell Signaling Technology), Cleaved Caspase-3 Antibody (# 9664S, Cell Signaling Technology), GAPDH (14C10) Rabbit mAb (# 2118, Cell Signaling Technology) Anti VEGF Antibody (ab46154, Abcam), PD-L1/CD274 Monoclonal Antibody (66248-1, Proteintech).

Animal experiments

This study was conducted in accordance with the Declaration of Helsinki and approved by the Animal Ethics Committee of Lai 'an Technology (Guangzhou) Biology Co., LTD. (Agreement No. G2023003). All animal experiments were conducted in accordance with the Guidelines for the Welfare of Experimental Tumor Animals. Athymic nude mice (6–8 weeks old, male) or C57BL/6 mice (6–8 weeks old, male) were purchased from GemPharmatech. To evaluate the anti-tumor effect *in vivo*, unilateral subcutaneous implantation of cancer cell models was used. Among these models, 3×10^6 RM-1 cells, 1×10^6 GL261 cells with logarithmic growth phase were subcutaneously implanted into the right side of mice. When the tumor reached 50 mm^3–100 mm^3, each mouse was injected with OVM1 at a dose of 3×10^6 pfu (300 μL) per day through the tail vein for five consecutive injections. ABZ (50 mg/kg) was administered intraperitoneally every 2 days from the first day of OVM1 treatment. Under specific pathogen-free conditions, they maintained a standard diet and drank water freely throughout the entire experimental period. The tumor size of individual animals was continuously observed. The size of the subcutaneous tumor was measured using a digital caliper, and the tumor volume was calculated by multiplying the length by the second power of the width and then multiplying by 0.5. When the total volume of the tumor reached 2000 mm^3, the animal was euthanized by cervical dislocation. At the end of the experiment, mouse tumor tissue, spleen tissue, drained lymph nodes, and blood were collected for subsequent tests. For CD8+ T cell deletion, CD8 deletion antibody was intraperitoneally injected with a dose of 300 μg per mouse every 3 days from the day before day 1. For ICB therapy, CTLA4 targeting antibody was intraperitoneally injected at a dose of 200 μg per animal once every 3 days.

Immunoanalysis

The tumor tissue was separated into cells using a tumor dissociation kit (130-096-730, Mitenyi). The cells were then blocked with anti-mouse CD16/32 for 20 min. The cell suspension was stained with the following antibodies: mouse CD45-FITC (11-0451-85, Invitrogen), mouse CD3ε- Percp/Cyanine5.5 (100328, Biolegend), CD8 BV 421 (100737, Biolegend), CD4 APC eFluor 780 (47-0041-82, Invitrogen), CD44-PECy7 (103030, Biolegend), CD69-APC (104514, Biolegend), CD25-PE-Cy7 (101916, Biolegend), Foxp3-PE (12-5773-82, BD), ki67-BV650 (151215, Biolegend), CD11b APC eFluor 780 (47-0112-82, Invitrogen), F4/80-PE-Cy7 (25-4801-82, Invitrogen), CD80-BV650 (104731, Biolegend), CD163-APC (17-1631-82, Invitrogen), CTLA4 BV605 (106323, Biolegend), PD-L1-BV421 (124315, Biolegend), and PD1-PE (135206, Biolegend). Foxp3 and Ki67 in cells need to be fixed and broken before staining, while other antibodies can be directly stained. Samples were collected using Beckman Coulter CytoFLEX Flow Cytometer and data were analyzed using CytoExpert.

ELISA

Lymphocytes were separated from the spleen and draining lymph nodes using draining lymph node separation solution, and then cultured in 1640 medium containing 10% fetal bovine serum at 37°C. The next day, the lymphocytes were co-cultured with the corresponding tumor cells in a certain proportion. Forty-eight hours later, the supernatant was collected and the contents of cytotoxic factors secreted by lymphocytes were detected by mouse IFN-γ ELISA Kit (EK280/3–96, Multi Sciences), Mouse Granzyme B ELISA Kit (EK2173-96, Multi Sciences), and Mouse TNF-alpha ELISA Kit (EK282/4–96, Multi Sciences).

RT-qPCR

RNA was extracted from tumor tissue using Trizol. RNA is reverse-transcribed into cDNA using a reverse transcription kit (Thermo, EP0442). Then, using cDNA as template, FastReal fast quantitative PCR premixed reagent was used for real-time quantitative PCR detection (FP217-03, TIANGEN). The primers used were as follows:

mNS1-F:GTTCCAACAGGCGTCACCATC; mNS1-R:ACACATTC TTGTCTAGCACAGTCC; mGAPDH-F:CATCACTGCCACCCAG AAGACTG; mGAPDH-R: ATGCCAGTGAGCTTCCCGTTCAG; mCXCL9-F:ACGGAGATCAAACCTGCCTA; mCXCL9-R:TTTTC CCCCTCTTTTGCTTT; mCXCL10-F:AAGTGCTGCCGTCATTTT CT; mCXCL10-R:GTGGCAATGATCTCAACACG; mCXCL11-F:AG CTGCTCAAGGCTTCCTTA; mCXCL11-R:CTGCATTATGAGGC GAGCTT; mVEGF-F:ATTAACCATGTGCCCGAGAA; mVEGF-R:TCTTGCAAACTGCAGGAATG; mCD274-F:TGCTGCATAAT CAGCTACGG; mCD274-R:ATGCTCAGAAGTGGCTGGAT; mIL-12-F:GCAGTAGCAGTTCCCCTGAC; mIL-12-R:AGTCCCTTTGG TCCAGTGTG; mIFNG-F:GCGTCATTGAATCACACCTG; mIFNG-R:GACCTGTGGGTTGTTGACCT; mIL-6-F:CCGGAGAGGAGAC TTCACAG; mIL-6-R:CAGAATTGCCATTGCACAAC.

Gene expression was normalized to GAPDH and calculated using the $2^{-\Delta\Delta CT}$ method. The following conditions were used for the amplification. After a few minutes of pre-denaturation at 95°C, 40 cycles of 10 s of denaturation at 95°C, 30 s of annealing at 61°C, and one cycle of 30 s of denaturation at 95°C, 30 s of annealing at 60°C. Relative quantitation of mRNA was normalized by that of Actin as the internal control.

Data analysis

All data were statistically analyzed and plotted using Graphpad Prism 8.0 software. The quantitative data produced in this study conform to the normal distribution and homogeneity of variance expressed as mean ± standard deviation. The t test was used to compare the two groups of data. Tumor measurement curves were expressed as the means ± SD, where $p < 0.05$ is considered statistically significant, and * represents $p < 0.05$, ** $p < 0.01$, *** $p < 0.001$, **** $p < 0.0001$, and ns represents no statistically significant difference.

DATA AND CODE AVAILABILITY

All data have been presented in the manuscript.

SUPPLEMENTAL INFORMATION

Supplemental information can be found online at https://doi.org/10.1016/j.omton.2024.200813.

ACKNOWLEDGMENTS

This research was funded by National Key R&D Program of China (2021YFA0909800); National Natural Science Foundation of China (82073883); National Natural Science Foundation of China (82173837); Guangdong Basic and Applied Basic Research Foundation (2022B1515020056); National Natural Science Foundation of China (82173838); Fundamental Research Funds for the Central Universities, Sun Yat-sen University (23ykbj001). The author would like to thank Dr. Cui Guo and Dr. Weiwei Chu for their technical support, as well as Xiudan Zhan and Boning Zeng for their assistance in manuscript editing.

AUTHOR CONTRIBUTIONS

W.B. performed and analyzed the experiments. W.B. and J.H. designed the study. X.T., J.C., C.C., Y.L., X.L., T.X., Y.Q., X.T., and B.Z. helped to perform the experiments. W.B., W.Z., and G.Y. analyzed and interpreted data. J.H., J.L., J.C., and Y.L. secured funding. J.H., and J.L. supervised the project. W.B. and J.H. drafted the manuscript. All authors edited and approved the final manuscript.

DECLARATION OF INTERESTS

The authors declare no competing interests.

REFERENCES

1. Kaufman, H.L., Kohlhapp, F.J., and Zloza, A. (2015). Oncolytic viruses: a new class of immunotherapy drugs. Nat. Rev. Drug Discov. *14*, 642–662. https://doi.org/10.1038/nrd4663.

2. Hu, J., Cai, X.F., and Yan, G. (2009). Alphavirus M1 induces apoptosis of malignant glioma cells via downregulation and nucleolar translocation of p21WAF1/CIP1 protein. Cell Cycle *8*, 3328–3339. https://doi.org/10.4161/cc.8.20.9832.

3. Voron, T., Colussi, O., Marcheteau, E., Pernot, S., Nizard, M., Pointet, A.L., Latreche, S., Bergaya, S., Benhamouda, N., Tanchot, C., et al. (2015). VEGF-A modulates expression of inhibitory checkpoints on CD8+ T cells in tumors. J. Exp. Med. *212*, 139–148. https://doi.org/10.1084/jem.20140559.

4. Zhang, Y., and Brekken, R.A. (2022). Direct and indirect regulation of the tumor immune microenvironment by VEGF. J. Leukoc. Biol. *111*, 1269–1286. https://doi.org/10.1002/JLB.5RU0222-082R.

5. Pene, P., Mojon, M., Garin, J.P., Coulaud, J.P., and Rossignol, J.F. (1982). Albendazole: a new broad spectrum anthelmintic. Double-blind multicenter clinical trial. Am. J. Trop. Med. Hyg. *31*, 263–266. https://doi.org/10.4269/ajtmh.1982.31.263.

6. Ehteda, A., Galettis, P., Pillai, K., and Morris, D.L. (2013). Combination of albendazole and 2-methoxyestradiol significantly improves the survival of HCT-116 tumor-bearing nude mice. BMC Cancer *13*, 86. https://doi.org/10.1186/1471-2407-13-86.

7. Whittaker, C., Chesnais, C.B., Pion, S.D.S., Kamgno, J., Walker, M., Basáñez, M.G., and Boussinesq, M. (2022). Factors associated with variation in single-dose albendazole pharmacokinetics: A systematic review and modelling analysis. PLoS Neglected Trop. Dis. *16*, e0010497. https://doi.org/10.1371/journal.pntd.0010497.

8. Zhang, Q.L., Lian, D.D., Zhu, M.J., Li, X.M., Lee, J.K., Yoon, T.J., Lee, J.H., Jiang, R.H., and Kim, C.D. (2019). Antitumor Effect of Albendazole on Cutaneous Squamous Cell Carcinoma (SCC) Cells. BioMed Res. Int. *2019*, 3689517. https://doi.org/10.1155/2019/3689517.

9. Zhu, L., Kuang, X., Zhang, G., Liang, L., Liu, D., Hu, B., Xie, Z., Li, H., Liu, H., Ye, M., et al. (2022). Albendazole induces immunotherapy response by facilitating ubiquitin-mediated PD-L1 degradation. J. Immunother. Cancer *10*, e003819. https://doi.org/10.1136/jitc-2021-003819.

10. Zheng, B., Zhang, J., Chen, H., Nie, H., Miller, H., Gong, Q., and Liu, C. (2020). T Lymphocyte-Mediated Liver Immunopathology of Schistosomiasis. Front. Immunol. *11*, 61. https://doi.org/10.3389/fimmu.2020.00061.

11. Diaz-Zaragoza, M., Jimenez, L., Hernandez, M., Hernandez-Avila, R., Navarro, L., Ochoa-Sanchez, A., Encarnacion-Guevara, S., Ostoa-Saloma, P., and Landa, A. (2020). Protein expression profile of Taenia crassiceps cysticerci related to Th1- and Th2-type responses in the mouse cysticercosis model. Acta Trop. *212*, 105696. https://doi.org/10.1016/j.actatropica.2020.105696.

12. Zhou, F., Du, J., and Wang, J. (2017). Albendazole inhibits HIF-1alpha-dependent glycolysis and VEGF expression in non-small cell lung cancer cells. Mol. Cell. Biochem. *428*, 171–178. https://doi.org/10.1007/s11010-016-2927-3.

13. Cai, J., Lin, Y., Zhang, H., Liang, J., Tan, Y., Cavenee, W.K., and Yan, G. (2017). Selective replication of oncolytic virus M1 results in a bystander killing effect that is potentiated by Smac mimetics. Proc. Natl. Acad. Sci. USA *114*, 6812–6817. https://doi.org/10.1073/pnas.1701002114.

14. Liu, Y., Cai, J., Liu, W., Lin, Y., Guo, L., Liu, X., Qin, Z., Xu, C., Zhang, Y., Su, X., et al. (2020). Intravenous injection of the oncolytic virus M1 awakens antitumor T cells and overcomes resistance to checkpoint blockade. Cell Death Dis. *11*, 1062. https://doi.org/10.1038/s41419-020-03285-0.

15. Bronte, V., and Pittet, M.J. (2023). The Spleen in Local and Systemic Regulation of Immunity. Immunity *56*, 1152. https://doi.org/10.1016/j.immuni.2023.04.004.

16. Weiss, J.M., Subleski, J.J., Wigginton, J.M., and Wiltrout, R.H. (2007). Immunotherapy of cancer by IL-12-based cytokine combinations. Expet Opin. Biol. Ther. *7*, 1705–1721. https://doi.org/10.1517/14712598.7.11.1705.

17. Beyranvand Nejad, E., Labrie, C., van der Sluis, T.C., van Duikeren, S., Franken, K.L.M.C., Roosenhoff, R., Arens, R., van Hall, T., and van der Burg, S.H. (2021). Interleukin-6-mediated resistance to immunotherapy is linked to impaired myeloid cell function. Int. J. Cancer *148*, 211–225. https://doi.org/10.1002/ijc.33280.

18. Liu, W., Liu, Y., Hu, C., Xu, C., Chen, J., Chen, Y., Cai, J., Yan, G., and Zhu, W. (2021). Cytotoxic T lymphocyte-associated protein 4 antibody aggrandizes antitumor immune response of oncolytic virus M1 via targeting regulatory T cells. Int. J. Cancer *149*, 1369–1384. https://doi.org/10.1002/ijc.33703.

19. Menjivar, R.E., Nwosu, Z.C., Du, W., Donahue, K.L., Hong, H.S., Espinoza, C., Brown, K., Velez-Delgado, A., Yan, W., Lima, F., et al. (2023). Arginase 1 is a key driver of immune suppression in pancreatic cancer. Elife *12*. https://doi.org/10.7554/eLife.80721.

20. Niu, F., Yu, Y., Li, Z., Ren, Y., Li, Z., Ye, Q., Liu, P., Ji, C., Qian, L., and Xiong, Y. (2022). Arginase: An emerging and promising therapeutic target for cancer treatment. Biomed. Pharmacother. *149*, 112840. https://doi.org/10.1016/j.biopha.2022.112840.

21. Park, S.H., Kim, H., Kwak, S., Jeong, J.H., Lee, J., Hwang, J.T., Choi, H.K., and Choi, K.C. (2020). HDAC3-ERalpha Selectively Regulates TNF-alpha-Induced Apoptotic Cell Death in MCF-7 Human Breast Cancer Cells via the p53 Signaling Pathway. Cells *9*, 1280. https://doi.org/10.3390/cells9051280.

22. Wu, Z., Huang, H., Han, Q., Hu, Z., Teng, X.L., Ding, R., Ye, Y., Yu, X., Zhao, R., Wang, Z., and Zou, Q. (2022). SENP7 senses oxidative stress to sustain metabolic fitness and antitumor functions of CD8+ T cells. J. Clin. Invest. *132*, e155224. https://doi.org/10.1172/JCI155224.

23. He, X., and Xu, C. (2020). Immune checkpoint signaling and cancer immunotherapy. Cell Res. *30*, 660–669. https://doi.org/10.1038/s41422-020-0343-4.

24. Hemminki, O., Dos Santos, J.M., and Hemminki, A. (2020). Oncolytic viruses for cancer immunotherapy. J. Hematol. Oncol. *13*, 84. https://doi.org/10.1186/s13045-020-00922-1.

25. Omole, R.K., Oluwatola, O., Akere, M.T., Eniafe, J., Agboluaje, E.O., Daramola, O.B., Ayantunji, Y.J., Omotade, T.I., Torimiro, N., Ayilara, M.S., et al. (2022). Comprehensive assessment on the applications of oncolytic viruses for cancer immunotherapy. Front. Pharmacol. *13*, 1082797. https://doi.org/10.3389/fphar.2022.1082797.

26. Zolaly, M.A., Mahallawi, W., Khawaji, Z.Y., and Alahmadi, M.A. (2023). The Clinical Advances of Oncolytic Viruses in Cancer Immunotherapy. Cureus *15*, e40742. https://doi.org/10.7759/cureus.40742.

27. Liu, Y., Hu, C., Zhu, W.B., Xu, W.X., Li, Z.Y., Lin, Y., Cai, J., Liang, J.K., Zhu, X., Gao, Z.L., et al. (2018). Association of Low Zinc Finger Antiviral Protein Expression with Progression and Poor Survival of Patients with Hepatocellular Carcinoma. Cell. Physiol. Biochem. *49*, 1007–1018. https://doi.org/10.1159/000493285.

28. Cerullo, V., Pesonen, S., Diaconu, I., Escutenaire, S., Arstila, P.T., Ugolini, M., Nokisalmi, P., Raki, M., Laasonen, L., Särkioja, M., et al. (2010). Oncolytic adenovirus coding for granulocyte macrophage colony-stimulating factor induces antitumoral immunity in cancer patients. Cancer Res. *70*, 4297–4309. https://doi.org/10.1158/0008-5472.CAN-09-3567.

29. Eriksson, E., Milenova, I., Wenthe, J., Ståhle, M., Leja-Jarblad, J., Ullenhag, G., Dimberg, A., Moreno, R., Alemany, R., and Loskog, A. (2017). Shaping the Tumor Stroma and Sparking Immune Activation by CD40 and 4-1BB Signaling Induced by an Armed Oncolytic Virus. Clin. Cancer Res. *23*, 5846–5857. https://doi.org/10.1158/1078-0432.CCR-17-0285.

30. Huang, H., Langenkamp, E., Georganaki, M., Loskog, A., Fuchs, P.F., Dieterich, L.C., Kreuger, J., and Dimberg, A. (2015). VEGF suppresses T-lymphocyte infiltration in the tumor microenvironment through inhibition of NF-kappaB-induced endothelial activation. Faseb. J. *29*, 227–238. https://doi.org/10.1096/fj.14-250985.

31. Gavalas, N.G., Tsiatas, M., Tsitsilonis, O., Politi, E., Ioannou, K., Ziogas, A.C., Rodolakis, A., Vlahos, G., Thomakos, N., Haidopoulos, D., et al. (2012). VEGF directly suppresses activation of T cells from ascites secondary to ovarian cancer via VEGF receptor type 2. Br. J. Cancer *107*, 1869–1875. https://doi.org/10.1038/bjc.2012.468.

32. Sun, Q., Hong, Z., Zhang, C., Wang, L., Han, Z., and Ma, D. (2023). Immune checkpoint therapy for solid tumours: clinical dilemmas and future trends. Signal Transduct. Targeted Ther. *8*, 320. https://doi.org/10.1038/s41392-023-01522-4.

33. Topalian, S.L., Taube, J.M., Anders, R.A., and Pardoll, D.M. (2016). Mechanism-driven biomarkers to guide immune checkpoint blockade in cancer therapy. Nat. Rev. Cancer *16*, 275–287. https://doi.org/10.1038/nrc.2016.36.

34. Zheng, M. (2022). Tumor mutation burden for predicting immune checkpoint blockade response: the more, the better. J. Immunother. Cancer *10*, e003087. https://doi.org/10.1136/jitc-2021-003087.